Behaviour of geocell reinforced soft clay bed subjected to incremental cyclic loading

A. Hegde [*1], and T.G. Sitharam [2]

[1] *Department of Civil and Environmental Engineering, Indian Institute of Technology, Patna 801103, India*
[2] *Department of Civil Engineering, Indian Institute of Science, Bangalore 560012, India*

Abstract. The paper deals with the results of the laboratory cyclic plate load tests performed on the reinforced soft clay beds. The performances of the clay bed reinforced with geocells and geocells with additional basal geogrid cases are compared with the performance of the unreinforced clay beds. From the cyclic plate load test results, the coefficient of elastic uniform compression (C_u) was calculated for the different cases. The C_u value was found to increase in the presence of geocell reinforcement. The maximum increase in the C_u value was observed in the case of the clay bed reinforced with the combination of geocell and geogrid. In addition, 3 times increase in the strain modulus, 10 times increase in the bearing capacity, 8 times increase in the stiffness and 90% reduction in the settlement was observed in the presence of the geocell and geogrid. Based on the laboratory test results, a hypothetical case of a prototype foundation subjected to cyclic load was analyzed. The results revealed that the natural frequency of the foundation-soil system increases by 4 times and the amplitude of the vibration reduces by 92% in the presence of the geocells and the geogrids.

Keywords: geocells; cyclic plate load test; coefficient of elastic uniform compression; natural frequency; bearing capacity

1. Introduction

The foundation beds are often subjected to cyclic loads due to many circumstances, such as earthquakes, traffic loads, and the machine vibrations in the case of the machine foundations. These cyclic loads are generally smaller as compared to the static loads; but are repetitive. As a result of these cyclic forces, the soil bed may undergo large settlements and subsequently may fail to support the superstructure above. In order to resist the cyclic stresses, generally, stiffness of the soil is increased. Out of many available techniques, soil reinforcement technique using geosynthetics is the most sought after technique to increase the stiffness of the soil (Dash *et al*. 2001a, Sitharam and Sireesh 2004, Hegde and Sitharam 2015a). Earlier days, geogrids were used to reinforce the soil. However, more effective and promising way of reinforcing the soil is to use the geocells (Hegde and Sitharam 2013, Hegde and Sitharam 2015b).

Geocells are 3-dimensional expandable panels made up of ultrasonically welded high strength

---

∗Corresponding author, Assistant Professor, E-mail: amarnathhegde@gmail.com
[a] Professor, E-mail: sitharam@iisc.ernet.in

polymers or the polymeric alloy such as Polyethylene, Polyolefin etc. Geocells are being widely used in the geotechnical engineering. General applications of the geocells include foundations, embankments, pavements, and retaining structures. Many researchers have highlighted the beneficial use of geocells and its efficacy in increasing the stiffness of the soil (Madhavi Latha and Somawanshi 2009, Pokharel *et al*. 2010, Tanyu *et al*. 2013, Sitharam and Hegde 2013, Sireesh *et al*. 2013, Leshchinsky and Ling 2013, Dash and Bora 2013, Hegde *et al*. 2014, Hegde and Sitharam 2015c). By virtue of its 3-dimensional nature, it offers additional confinement to the soil and hence, helps to improve the overall performance of the foundation bed (Hegde and Sitharam 2015d, e).

Generally, the performances of the foundation bed get affected due to the action of continuous cyclic stresses. In such cases, the performance can be enhanced in two ways. One way is to increase the stiffness of the soil to resist the cyclic stresses. The other approach is to increase the elasticity of the soil. With the increase in the elasticity of the soil, the soil will regain its original position before the next cycle of cyclic stress is applied. This will lead to the lesser permanent deformation of the foundation bed. Generally, rubber pads, cork sheets and the spring coils are used below the foundations to increase the elastic properties of the soil (Srinivasalu and Vaidyanathan 1976, IS 13301 1992, Bhatia 2008). As highlighted before, the use of the geocells to increase the stiffness of the soil has been demonstrated by many researchers. The present study focuses on the aspect of increasing the elasticity of the soil using the geocell reinforcement. This particular concept has not been explored very well in the past.

Basically, coefficient of elastic uniform compression (C_u) is the measure of the elastic modulus of the soil. It is defined as the ratio of the compressive stress (P) applied to the soil to the elastic part of the settlement (S_e) induced. Generally, it is determined from the cyclic plate load tests.

$$C_u = P / S_e \qquad (1)$$

Higher value of C_u indicates the high elastic modulus of the soil. By knowing the value of the coefficient of elastic uniform compression, the other soil elastic constants can be calculated using the relations listed in Table 1. These soil constants are used in the design of the machine foundations subjected to different modes of vibration.

Moghaddas Tafreshi *et al*. (2008) studied the effect of relative density of the sand bed on the coefficient of elastic uniform compression and found that the C_u value increases with the increase in relative density. Verma and Bhatt (2008) performed cyclic plate load tests on geogrid reinforced sand beds and observed the increment in the coefficient of elastic uniform compression in the presence of geogrid. Similar observations were also made by Sreedhar and Goud (2011). The aim of the research is to study the effect of geocell reinforcement on the value of elastic uniform compression in the soft soil. Hence, laboratory cyclic plate load tests were performed on the

Table 1 Elastic constants to be used for different modes of vibration

Mode of vibration	Elastic constants used in the design	Relation
Vertical mode of vibrations	Coefficient of elastic uniform compression (C_u)	-
Translational mode of vibration	Coefficient of elastic uniform shear (C_τ)	$C_\tau = 0.5 C_u$
Rotational mode of vibrations	Coefficient of elastic, non-uniform compression (C_φ)	$C_\varphi = 2 C_u$
Torsional mode of vibrations	Coefficient of elastic non-uniform shear (C_ψ)	$C_\psi = 0.75 C_u$

unreinforced and geocell reinforced soft clay beds. In addition to geocell, the combination of geocell and geogrid reinforced case was also studied. The tests conducted were conforming to IS 5249 (1992) and DIN 18134 (2001).

2. Experimental studies

2.1 Experimental setup

A cast iron test tank of 900 mm long, 900 mm wide and 600 mm in height was used in the experimental investigation. The tank was connected to the loading frame and which was internally connected to manually operated hydraulic jack. A 20 mm thick square steel plate with width 150 mm was used as the loading plate. The loading plate was selected in such a way that, its width was equal to 1/6th of the width of the tank in order to avert the boundary effects. The bottom of the plate was made rough by coating a thin layer of sand with epoxy glue. The load was applied to the plate through the hydraulic jack. A pre-calibrated proving ring was placed between the plate and hydraulic jack to measure the applied load. A ball bearing arrangement was used to prevent the eccentric application of the load. Figs. 1(a)-(b) represents the schematic and the photographic view of the test setup.

2.2 Materials used

Natural silty clay with specific gravity 2.66 was used to prepare the foundation bed. The liquid limit and the plastic limit of the clay were 40% and 17% respectively. As per Unified Soil Classification System, clay was classified as clay with low to medium plasticity (CL). The maximum dry density and the optimum moisture content of the soil in the Standard Proctor test were 18.2 kN/m^3 and 13.2% respectively. Dry sand was used to fill the geocell pockets. Sand was having specific gravity 2.64, effective particle size (D_{10}) 0.26 mm, coefficient of uniformity 3.08,
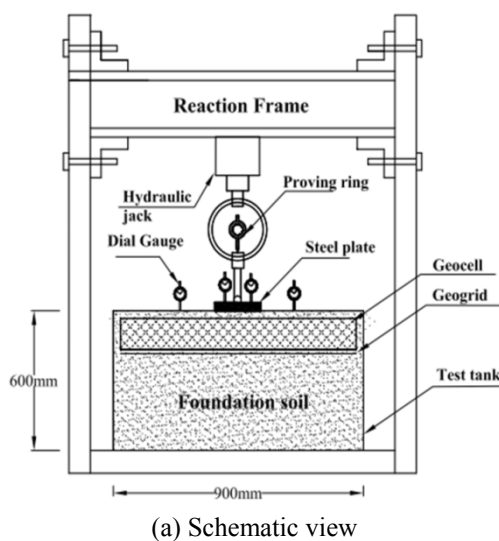

(a) Schematic view   (b) Photographic view
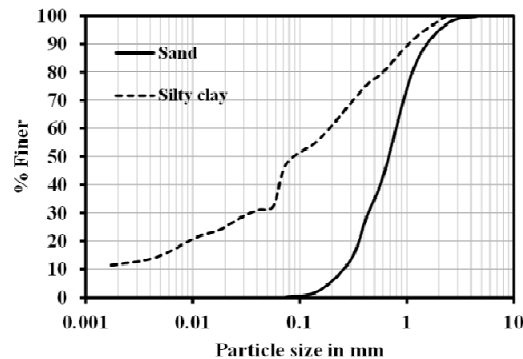
Fig. 1 Test setup

Fig. 2 Grain size distribution of the material

coefficient of uniformity (C_c) 1.05, maximum void ratio (e_{max}) 0.81, minimum void ratio (e_{min}) 0.51 and angle of internal friction (φ) 36°. As per Unified Soil Classification System, the sand was classified as poorly graded sand with symbol SP. The grain size distribution of both sand and clay are shown in Fig. 2.

The commercially available Neoloy geocells were used in the study. The 'Neoloy' is a polymeric alloy composed of polyolefin and thermoplastic polymer. These geocells are known for high strength and durability. The strip thickness and the aspect ratio of the geocell used in the study were 1.53 mm and 0.6 respectively. The geocell had a unique texture on its surface. The modified direct shear test was conducted to study the interaction between the geocell and the sand (Srinivasa Murthy *et al*. 1993). The interface friction angle value of 30° was observed between the geocell and the sand. The surface roughness of the geocell was estimated using the optical profilometer. The surface roughness value of 1.12 μm was observed (Hegde and Sitharam 2015f).

Table 2 Properties of the geocell and geogrid

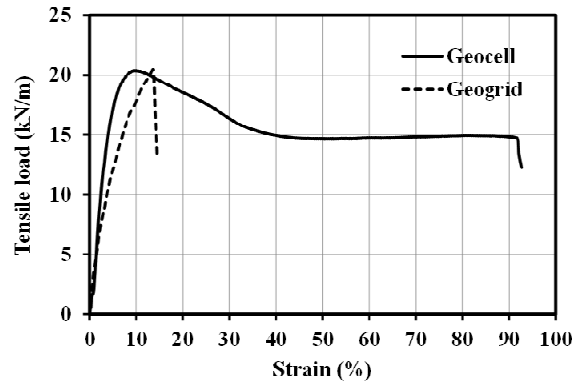| Parameters	Quantity
Geocell	
Material	Neoloy
Aspect ratio	0.6
No. of cells/m^2	40
Cell depth (mm)	150
Strip thickness (mm)	1.53
Cell seam strength (N)	2150 ($\pm$ 5%)
Density (g/cm^3)	0.95 ($\pm$ 1.5%)
Ultimate tensile strength (kN/m)	20
Geogrid	
Polymer	Polypropylene
Aperture size (MD × XMD) mm	35 × 35
Ultimate tensile strength (kN/m)	20
Mass per unit area (g/m^2)	220
Shape of aperture opening	Square

Fig. 3 Tensile load-axial strain behavior of geocell and geogrid

Below the geocell, a layer of biaxial geogrid made of Polypropylene was used. The aperture opening of the geogrid was square in shape with size 35 mm × 35 mm. The summary of the properties of the geocell and geogrids are presented in Table 2. The tensile strength of the geocell and the geogrid were determined as per the guidelines of ASTM D-4885 and ASTM D-6637 respectively. The tensile stress-strain behaviors of the geocell and geogrid are shown in Fig. 3.

2.3 Preparation of clay bed

Firstly, the air-dried clay was powdered and mixed with the predetermined amount of water. The moist soil was placed in the airtight container for 3-4 days for allowing uniform distribution of moisture within the sample before kneading it again. The sides of the tank were covered with polyethylene sheets to minimize the side friction. Foundation bed of 400 mm thick was prepared by compacting the soil uniformly in layers of 25 mm each. A manually operated plate compactor was used for the compaction. By carefully controlling the compaction effort and the water content of the test bed, a uniform density condition was maintained in all layers. The fall cone apparatus was used to measure the undrained cohesion values at different locations during different stages of the bed preparation. The fall cone apparatus provides rapid and accurate measurement of undrained shear strength (Zreik *et al*. 1985). An undrained cohesion value of 5 kPa was maintained in all the tests. Undisturbed samples were collected at different locations of the test bed to determine the degree of saturation, unit weight, moisture content and the undrained shear strength of the soil mass. Properties of the clay bed are summarized in Table 3 and the same properties were maintained in all the three tests. Clay bed was freshly prepared from the dry soil for the every new test. Both geocell and geogrid were placed to the full width of the tank. Dash *et al*. (2001b) reported that the optimum depth of placement of geocell is 0.1*B* from the bottom of the footing (where '*B*' is the width of the steel plate). Hence, in the present investigation, the geocell was placed at the depth of 0.1*B* below the steel plate. The geogrid was placed below the geocells. The geocell pockets were filled up with the clean sand using the pluviation technique to achieve the relative density of 65%. Before the start of the pluviation, a series of trials were conducted to determine the height of fall required to achieve the desired relative density. In each trial, small aluminum cups with known volume were placed at the different locations of the geocell pocket. By knowing the maximum and minimum void ratios of the sand, a calibration chart was prepared. The height of fall required to achieve 65% relative density was directly obtained from the chart.

Table 3 Properties of the soft clay bed

Parameters	Values
Moisture content (%)	26
Unit weight (kN/m^3)	18.63
Dry unit weight (kN/m^3)	14.81
Undrained shear strength (kPa)	5

The pluviation was continued up to a thickness of 15 mm above the geocell pockets. A layer of geotextile was used as the separator between soft clay bed and the sand overlaying it. Upon filling the geocell with the sand, the fill surface was leveled.

2.4 Testing procedure

Loading plate was placed at the top of the bed at a pre-determined alignment. Through the precise measurements, the plate was placed at the centre such that, it rests on three adjacent pockets of the geocells. Two dial gauges (D_1 and D_2) were placed on the either side of the center line of the plate to record the plate settlements. Another set of dial gauges (S_1 and S_2) was placed at the distance of 1.5B (B is the width of the plate) from the center line of the plate to measure the deformation underwent by the fill surface. Figs. 4(a)-(b) shows the photographs of the model preparation and testing.

Once the test setup was ready, the initial readings of the dial gauges were noted and the first increment of static load was applied onto the plate. This load was maintained constant throughout for a period until no further settlement occurred or the rate of settlement became negligible. The final readings of the dial gauges were then recorded. The entire load was then removed gradually and the plate was allowed to rebound. When no further rebound was occurred or the rate of rebound became negligible, the readings of the dial gauges were again noted. The load was then increased gradually till its magnitude acquires a value equal to the proposed next higher stage of loading. The load was maintained constant and the final dial gauge reading was noted as mentioned earlier. The entire load was then reduced to zero and final dial gauge readings were
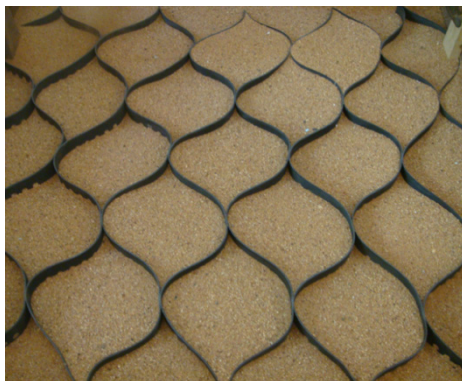
| (a) Partially filled geocells | (b) Reinforced bed before the test |

Fig. 4 Photographs of the model preparation and testing

recorded when the rate of rebound becomes negligible. The cycles of loading, unloading and reloading were continued till the estimated ultimate load was reached. Each time, the final values of dial gauge readings were noted.

3. Results and discussion

Figs. 5(a)-(c) represents the bearing pressure-settlement response for the three different cases, namely, unreinforced, geocell reinforced and geocell with additional basal geogrid reinforced respectively. In case of the unreinforced bed, the failure occurred in 3rd load increment itself. The failure of the bed was indicted by the large settlement of the plate. The maximum bearing capacity of 28 kPa was observed. In case of the geocell reinforced case and the geocell with additional basal geogrid case, the test was stopped after 7th load increments as there was no failure of the bed. In all the 3 cases, every loading cycle was followed by a gradual unloading of the entire load. The elastic rebound of the plate was recorded for every loading and unloading cycle.

After the tests, the infill soil was scooped out and geocell was removed. Figs. 6(a)-(b) represents the photograph of the geocell before and after the tests. Post-test geocell has shown the deformation in the vertical and horizontal ribs due to the action of the cyclic loading. In addition to the loaded cell, the deformation was also observed in the surrounding cells. Hence, it is evident that, all the interconnected cells in the geocells act together like a large mat that spreads the applied load over the larger area, leading to the overall improvement in the performance of the foundation beds (Dash *et al*. 2001b, Hegde and Sitharam 2015g).

From the bearing pressure-settlement response, the strain moduli for first and second cycle
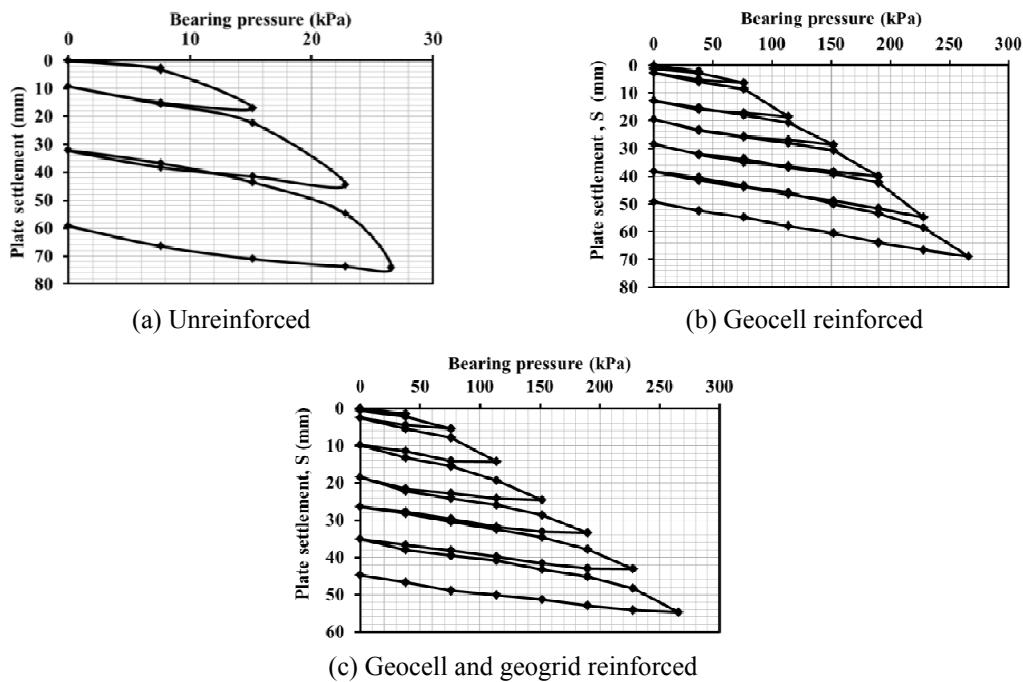

(a) Unreinforced

(b) Geocell reinforced

(c) Geocell and geogrid reinforced

Fig. 5 Bearing pressure-settlement responses

(a) Before the test   (b) After the test

Fig. 6 Photograph of the geocell

were calculated as per the guidelines of DIN 18134 (2001) for different cases. Basically, the strain modulus is the indication of the elastic modulus of the bed. In order to determine the strain moduli, the load settlement curve should be smooth. The settlement (S) at the centre of the loading plate is expressed as the function of the average normal stress (σ_o) below the plate.

$$S = a_0 + a_1.\sigma_o + a_2.\sigma_o^2 \tag{2}$$

where a_o, a_1, a_2 are the constants. For determining these factors, the following equations were used. The value of settlement 'S' equal to zero was ignored in the calculation.

$$a_0.n + a_1 \sum_{i=1}^{n} \sigma_{oi} + a_2 \sum_{i=1}^{n} \sigma_{oi}^2 = \sum_{i=1}^{n} S_i \tag{3}$$

$$a_0 \sum_{i=1}^{n} \sigma_{oi} + a_1 \sum_{i=1}^{n} \sigma_{oi}^2 + a_2 \sum_{i=1}^{n} \sigma_{oi}^3 = \sum_{i=1}^{n} S_i.\sigma_{oi} \tag{4}$$

$$a_0 \sum_{i=1}^{n} \sigma_{oi}^2 + a_1 \sum_{i=1}^{n} \sigma_{oi}^3 + a_2 \sum_{i=1}^{n} \sigma_{oi}^4 = \sum_{i=1}^{n} S_i.\sigma_{oi}.\sigma_{oi}^2 \tag{5}$$

The strain modulus, E_v can be calculated using the relation.

$$E_v = \frac{1.5 \times r}{a_1 + a_2.\sigma_{o\max}} \tag{6}$$

where 'r' is the radius of the loading plate; $\sigma_{o\max}$ is the maximum average normal stress. The ratio of the strain modulus for the second and first cycles i.e., E_{v2}/E_{v1} are tabulated in the Table 4. The subscripts '1' and '2' indicates the respective number of cycles. The ratio of the strain modulus (E_{v2}/E_{v1}) found to increase in the presence of reinforcement. Maximum value was obtained in the presence of geocell and geogrid. Higher the value of E_{v2}/E_{v1} ratio indicates the higher elastic modulus of the soil. When the soil bed is reinforced with the geocells or the combination of geocells and geogrids, it forms a composite mass with the infill soil. The modulus of the composite

Table 4 Ratio of strain moduli for different cases

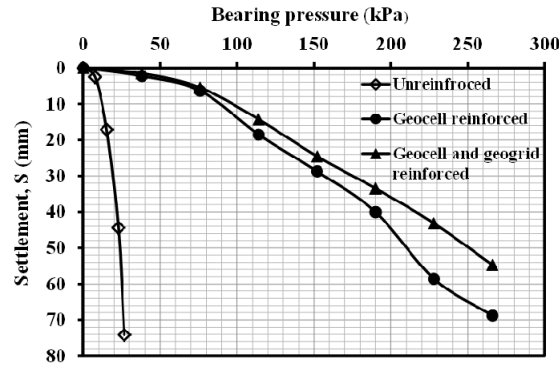|	Test cases		
Properties	Unreinforced	Geocell reinforced	Geocell+Geogrid reinforced
E_{v2}/E_{v1}	14.7	36	45

Fig. 7 Static bearing pressure-settlement envelope

mass is always higher than the soil alone. The similar observations were also made by Bathurst and Karpurapu (1993) and Rajagopal *et al.* (1999).

The advantage of the cyclic plate load test is that, it not only provides the information about the elastic properties of the soil, but also provides information about bearing capacity and the settlement of the bed. From the cyclic bearing pressure-settlement response, it is also possible to obtain the static boundary of the bearing pressure-settlement response of the plate as per IS 5249 (1992). For every loading cycle, by plotting the peak load against the corresponding peak plate settlement, it is possible to obtain the static boundary of the pressure - settlement envelope as shown in Fig. 7. The static boundary of the pressure- settlement response obtained from the cyclic plate load test is not necessarily same as that of the pressure settlement response of the static plate load test. The pressure-settlement response of the reinforced soil bed is the function of the rate of loading. For unreinforced case, steep reduction in the pressure-settlement response was observed, indicating the failure of the bed. In case of geocell reinforcement, no clear cut failure was observed in the pressure-settlement behavior even up to the large settlement. The geocell mattress by virtue of its high bending and shear stiffness, supports the plate even after the failure of soil. It was observed that the provision of the additional geogrid layer at the base of the geocell mattress further increases the load carrying capacity as well as the stiffness of the clay bed (i.e., flattened pressure settlement curve).

Further, from the static pressure-settlement response, the bearing capacity improvement factor (I_f) was calculated. The bearing capacity improvement factor quantifies the improvement in the bearing capacity of the foundation bed due to the provision of the reinforcement. I_f is defined as below

$$I_f = \frac{q_r}{q_o} \tag{7}$$

where, q_r is the bearing pressure of the reinforced soil at the given settlement and q_0 is the bearing
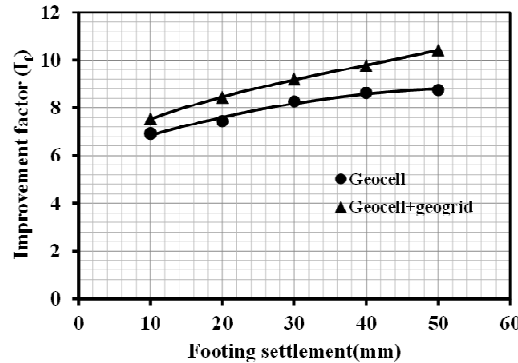
Fig. 8 Variation of bearing capacity improvement factor with plate settlement

pressure of unreinforced soil at the same settlement. Binquet and Lee (1975) reported the improvement factor is similar to the bearing capacity ratio. When the ratio is beyond the ultimate bearing capacity of the unreinforced soil, the ultimate bearing capacity (q_{ult}) is used instead of q_0. Variations of bearing capacity improvement factors with the plate settlement for different tests are shown in Fig 8. The I_f value found to increase with the increase in plate settlement. The maximum value of I_f i.e., $I_f = 10$ was observed in the case of combination of geocell and the geogrid. $I_f = 10$ means, 10 times increment in the load carrying capacity of the foundation bed as compared to the unreinforced bed.

The performance improvement of the foundation bed due to geocell reinforcement can also be quantified in terms of the reduction in the settlement of the bed using the parameter called percentage reduction in settlement (PRS). PRS is defined as

$$PRS = \left(\frac{S_O - S_r}{S_O} \right) \times 100 \tag{8}$$

where, S_o is settlement of the unreinforced foundation bed corresponding to its ultimate bearing capacity. The double tangent method (Vesic 1973) was used to estimate the ultimate load bearing capacity of the unreinforced clay bed. As per this method, the ultimate bearing capacity is defined as the pressure corresponding to the intersection of the two tangents; one at the early part of the pressure settlement curve and the another at the latter part. S_r is settlement of reinforced foundation bed corresponding to the bearing pressure equal to the ultimate bearing pressure of unreinforced foundation bed. The PRS values obtained for the geocell reinforced case and the combination of geocell and geogrid reinforced cases are listed in Table 5. Maximum value of PRS = 85% was observed for the clay bed reinforced with the combination of geocell and geogrid. PRS = 85%

Table 5 PRS and K_s values of the sand bed for different cases

Properties	Test cases		
	Unreinforced	Geocell reinforced	Geocell+Geogrid reinforced
PRS (%)	-	76	85
Subgrade reaction K_s (kN/m^3)	2992	16470	25333

means, 85% reduction in the settlement of the reinforced bed as compared to the unreinforced clay bed.

The stiffness of the foundation bed can also be estimated in terms of modulus of subgrade reaction (K_s). Modulus of subgrade reaction represents the stiffness of the soil bed at lower settlements. It is defined as the pressure corresponding to the 1.25 mm settlement in the load settlement behavior (DIN 18134 2001). Mathematically, K_s can be represented as

$$K_s(kN/m^3) = \frac{q_{1.25}(kPa)}{1.25 \times 10^{-3}}$$

(9)

where, $q_{1.25}$ is the uniform pressure applied to the plate at 1.25 mm of settlement. Generally, the modulus of subgrade reaction is used in the design of roads and airfield pavements. The K_s value calculated for different cases are listed in Table 5. The stiffness of the foundation bed found to increase due to the provision of the reinforcement. The maximum increment in the stiffness about 8 times was observed when the foundation bed was reinforced with combination of geocell and geogrid.

From the cyclic pressure-settlement response, the elastic rebound was calculated for each case. The elastic rebound was plotted against the bearing pressure for the different test cases as shown in Figs. 9(a)-(c). The slope of the line gives the elastic uniform compression (C_u). From the elastic uniform compression, the other elastic constants were determined. These elastic constants are used in the design of the machine foundations. Barkan (1962) proposed the methodology for the design of the machine foundations based on the concept of subgrade reaction. Table 6 lists the value of different elastic constants calculated from the (C_u). The elastic constants were found to increase in the presence of geocells. About 8 times increase in the C_u value was observed in the case of geocells. With the provision of basal geogrid, further increase in the C_u value (about 12 times) was observed.

4. Application of the study

It is known that the elastic uniform compression plays a significant role in the design of foundations subjected to cyclic loads e.g., machine foundations. The study suggested that the provision of the geocell helps to increase the coefficient of elastic uniform compression of the soil. In this regard, to explore the possibility of using the geocells in supporting the machine foundations, a hypothetical case has been analyzed. Before the analysis, the general procedure adopted in the design of machine foundation has been briefly discussed.

In the design of the machine foundations, the major principle is to avoid the resonance. Resonance occurs when the operating frequency of the machine matches with the natural frequency of the foundation-soil system. In order to avoid the resonance, the natural frequency (ω_n) of the foundation-soil system should be very large or very small compared to the operating frequency of the machines (ω). For low frequency machines generally, $\omega/\omega_n \leq 0.5$ and for the high frequency machines, $\omega/\omega_n \geq 1.5$. Generally, machines with frequency up to 1500 RPM are classified as the low frequency machines. Most of the reciprocating machines will have the operating frequency less than 1500 RPM and can be classified as the low frequency machines. The natural frequency of the foundation-soil system can be computed using the equation given Barkan (1962)
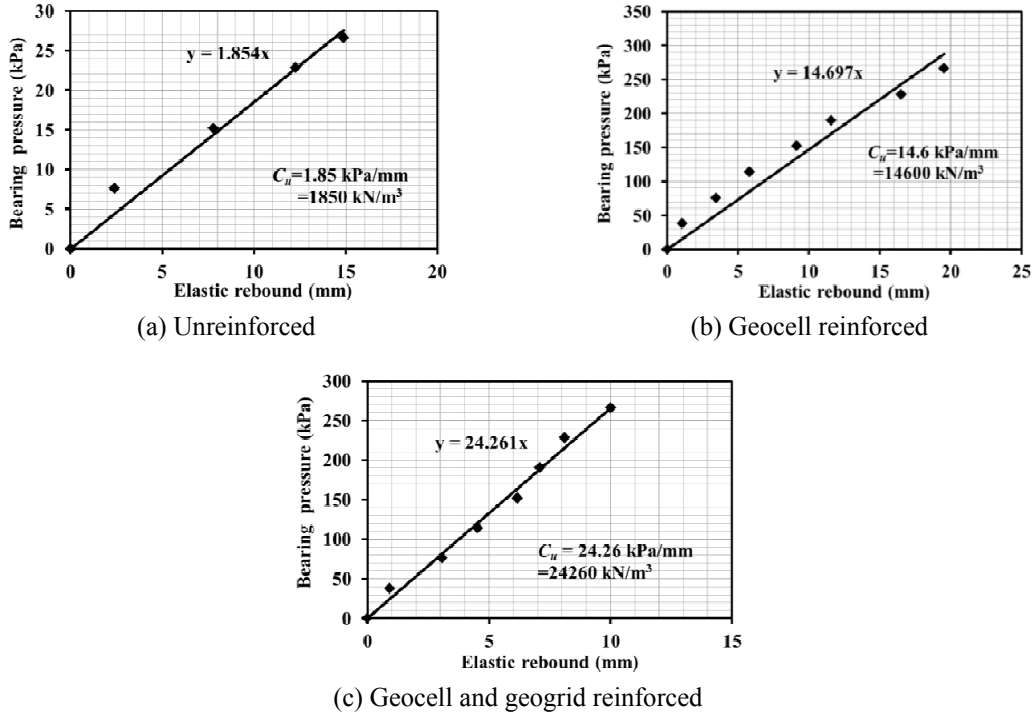
(a) Unreinforced

(b) Geocell reinforced

(c) Geocell and geogrid reinforced

Fig. 9 Bearing pressure vs. elastic rebound

Table 6 Comparison of elastic soil constants for different cases

Parameter	Unreinforced	Geocell reinforced	Geocell and geogrid reinforced
Coefficient of elastic uniform compression, C_u (kN/m³)	1850	14600	24260
Coefficient of elastic uniform shear, C_τ (kN/m³)	925	7300	12130
Coefficient of elastic non-uniform compression, C_φ (kN/m³)	3700	29200	48520
Coefficient of elastic non-uniform shear, C_ψ (kN/m³)	1387.5	10950	18195

$$\omega_n = \sqrt{\frac{C_u A}{m}} \tag{10}$$

where, C_u is the coefficient of elastic uniform compression; A is the cross sectional area of the plate; m is the mass of the foundation system cum the machine assembly. Generally, the natural frequency is controlled by controlling the mass and the base area of the foundation soil system. In case of high frequency machines, additional counterweights are placed on the foundation to reduce the natural frequency of the system. Similarly, in low frequency machines, the base area of the foundation is increased to increase the natural frequency of the foundation-soil system. However, the present approach emphasizes on increasing the coefficient of elastic uniform compression (C_u) to increase the natural frequency of the foundation-soil system.

For a particular foundation, it is evident from the Eq. (10) that the natural frequency (w_n) is

proportional to $\sqrt{C_u}$. In the present case, due to the presence of geocell and geogrid, the C_u value increases by 12 times as compared to unreinforced beds (refer Table 6). It means, the natural frequency increases by 3.5 times. Further, the amplitude of vibration of the foundation-soil system (A_z) for the un-damped case is calculated using Eq. (11)

$$ A_z = \frac{Q_o}{m(\omega_n^2 - \omega^2)} \tag{11} $$

where, Q_o is the magnitude of the cyclic force, From the Eq. (11), it is evident that the amplitude of vibration varies inversely with the natural frequency of the foundation soil system. As the natural frequency increases, the amplitude of vibration decreases. As the amplitude of the vibration reduces, the damage caused to the foundation due to the cyclic loading also reduces. The above mentioned concept has been demonstrated with a hypothetical case given below.

4.1 Demonstration

In this section, two hypothetical cases of machine foundation are compared. In the first case, the foundation was assumed to be resting on the unreinforced clay bed and in the second case, it was assumed to be resting on the geocell and geogrid reinforced clay beds. Further, a low frequency reciprocating machine was assumed to be placed on the foundation in both the cases. It should be noted that the hypothetical case considered has nothing to do with the model size and the loading conditions adopted in the laboratory tests. Here, the emphasis is only on the coefficient of elastic uniform compression. For the sake of convenience, the C_u values obtained from the model tests were used. Fig. 10 represents the schematic view of the hypothetical machine foundation resting on the geocell and geogrid reinforced clay bed. The following details were assumed.

The foundation dimension: 3 m × 3 m × 0.5 m
Cross-sectional area of the foundation (A): 9 m^2
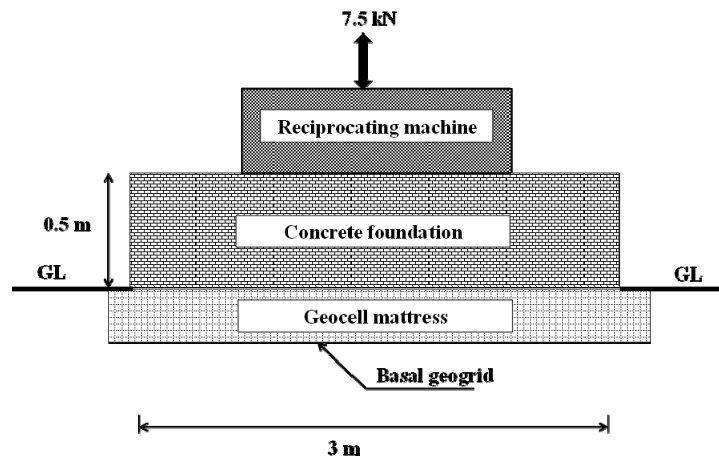Foundation material: Concrete with unit weight 24 kN/m^3

Fig. 10 Schematic view of the geocell supported machine foundation

Weight of the foundation: 24 × 3 × 3 × 0.5 = 108 kN
Weight of the machine = 42 kN (40% of the weight of the foundation as per Murthy, 2007).
Weight of the machine + foundation = 150 kN
Mass of the machine + foundation (m) = 15.2 kN-sec^2/m
Magnitude of the unbalance d force (Q_0) = 7.5 kN (5% of the weight of the machine + foundation)

The step by step calculations for the determination of the amplitude of vibration for the two different cases are tabulated in Table 7. The amplitude of the vibration (A_z) decreases in the presence of geocell reinforcement. About 87% reduction in the A_z value was observed in case of geocells and about 92% reduction in A_z was observed in the case of geocell with basal geogrid.

5. Scaling issues

The results of the small scale model tests are prone to scale effects. As suggested by Fakher and Jones (1996), the results of the model tests can be extrapolated to prototype cases by carefully applying the scaling laws. If '*N*' is the scaling factor, then the tensile strength of the geocell and geogrid to be used in the prototype application is N^2 times the tensile strength of the geocell and geogrid used in model tests (Viswanadham and König 2004, Sireesh *et al.* 2009). In model studies, commercial geocells and geogrids with tensile strength of 20 kN/m were used. Hence, the extrapolated results can be applicable to limited prototype applications. The present results can be extrapolated to a prototype case with scaling factor (*N*) value maximum up to 2. For *N* = 2, the tensile strength of the prototype geocell material becomes equal to of 80 kN/m. Generally, bamboo has the tensile strength in the range of 80 kN/m to 90 kN/m. The 3D cells and planar grids

Table 7 Calculation of the amplitude of vibration for different cases

Sl. No	Parameter	Unreinforced	Geocell reinforced	Geocell and geogrid reinforced
1	Coefficient of elastic uniform compression, C_u (kN/m^3) (From Table 6)	1850	14600	24260
2	Natural frequency of the foundation soil system, ω_n (rad/s) $\omega_n = \sqrt{\dfrac{C_u A}{m}}$	33	92	119
3	Natural frequency of the foundation soil system, ω_n (RPM)	314	881	1135
4	Limiting operating frequency of the machine, ω (rad/s), $\omega = 0.5 \times \omega_n$	16.5	46	60
5	Limiting operating frequency of the machine, ω (RPM)	157	440	568
6	Amplitude of vibration neglecting damping, (m) $A_z = \dfrac{Q_o}{m(\omega_n^2 - \omega^2)}$	6E-4	7.6E-5	4.58E-5
7	Reduction in the amplitude of vibration (%)	-	87	92

prepared from bamboo known as "bamboo cells" and "bamboo grids" could be used in the place of geocells and geogrids in prototype applications.

It is advised to carry out the chemical treatment of the bamboo using impregnation techniques to increase the durability. The further details of bamboo cells /bamboo grids and their application in soft soils have been explained elsewhere Hegde and Sitharam (2014f). In spite of the limitations, the 1-g model tests carried out in the present study are successful enough to highlight the efficacy of the geocells. The presented results are helpful to understand the basic mechanism and overall trends in the results. These results could be used for providing guidelines for design and construction of geocell-reinforced foundations, conducting large-scale model tests, and developing the analytical models.

6. Conclusions

This study highlights the efficacy of the geocells under the action of cyclic loading. Laboratory cyclic plate load tests were performed as per the guidelines of the IS 5249 (1992) and DIN 18134 (2001). The three different cases, namely, unreinforced, geocell reinforced and geocell with additional basal geogrid reinforced cases were considered. The coefficient elastic uniform compression (C_u) was evaluated from the cyclic plate load tests for the different cases. The C_u value was found to increase in the presence of reinforcements. Maximum improvement in the C_u value was observed in the case of the clay bed reinforced with the combination of geocell and geogrid. With the increase in the C_u value, the natural frequency of the foundation-soil system was increased and which resulted in the reduction of the amplitude of vibration. As the amplitude of the vibration reduces, the damage caused to the foundation due to the cyclic loading also reduces. In addition, 3 times increase in the strain modulus, 10 times increase in the bearing capacity, 8 times increase in the stiffness and 90% reduction in the settlement was observed in the presence of the geocell and geogrid. In this way, the study heighlight the possible new applications of geocells in supporting the foundation subjected to cyclic forces. In case of machine foundations, the findings are applicable for the case of the low frequency reciprocating machines, where the condition $\omega / \omega_n \leq 0.5$ is valid. It should be noted that the results of the 1-g model tests are subjected to scale effects. Hence, further studies in the form of centrifuge model studies or the large scale field tests are recommended to ascertain the findings.

References

ASTM D-4885 (2011), Standard test method for determining performance strength of geomembranes by wide strip tensile method; ASTM International, West Conshohocken, PA, USA.

ASTM D-6637 (2011), Standard test method for determining the tensile properties of geogrid by the single or multi-rib tensile method; ASTM International, West Conshohocken, PA, USA.

Barkan, D.D. (1962), *Dynamics of Bases and Foundations*, McGraw Hill Book Co., Inc., New York, NY, USA.

Bathurst, R.J. and Karpurapu, R. (1993), "Large scale triaxial tests on geocell reinforced granular soils", *Geotech. Test. J.*, **16**(3), 296-303.

Bhatia, K.G. (2008), "Foundations for industrial machines and earthquake effects", *ISET J. Earthq. Technol.*, **45**(1-2), 13-29.

Binquet, J. and Lee, L.K. (1975), "Bearing capacity tests on reinforced earth slabs", *J. Geotech. Eng. Div.*, **101**(12), 1241-1255.

Dash, S.K. and Bora, M.C. (2013), "Improved performance of soft clay foundations using stone columns and geocell-sand mattress", *Geotext. Geomembr.*, **41**, 26-35.

Dash, S.K., Rajagopal, K. and Krishnaswamy, N.R. (2001a), "Strip footing on geocell reinforced sand beds with additional planar reinforcement", *Geotext. Geomembr.*, **19**(8), 529-538.

Dash, S.K., Krishnaswamy, N.R. and Rajagopal, K. (2001b), "Bearing capacity of strip plates supported on geocell-reinforced sand", *Geotext. Geomembr.*, **19**(4), 235-256.

DIN 18134 (2001), *Determining the Deformation and Strength Characteristics of Soil by Plate Loading Tests*, German standard, Berlin, Germany, 10772.

Fakher, A. and Jones, C.J.F.P. (1996), "Discussion on Bearing capacity of rectangular footings on geogrid reinforced sand", *J. Geotech. Eng.*, **122**(4), 326-327.

Hegde, A. and Sitharam, T.G. (2013), "Experimental and numerical studies on plates supported on geocell reinforced sand and clay beds", *In. J. Geotech. Eng.*, **7**(4), 347-354.

Hegde, A.M. and Sitharam, T.G. (2015a), "Effect of infill materials on the performance of geocell reinforced soft clay beds", *Geomech. Geoeng.*, **10**(3), 163-173.

Hegde, A. and Sitharam, T.G. (2015b), "Experimental and numerical studies on protection of buried pipelines and underground utilities using geocells", *Geotext. Geomembr.*, **43**(5), 372-381.

Hegde, A. and Sitharam, T.G. (2015c), "Joint strength and wall deformation characteristics of a single cell subjected to uniaxial compression", *Int. J. Geomech.*, **15**(5), 1-8.

Hegde, A. and Sitharam, T.G. (2015d), "3-Dimensional numerical modelling of geocell reinforced sand beds", *Geotext. Geomembr.*, **43**(2), 171-181.

Hegde, A.M. and Sitharam, T.G. (2015e), "3-Dimensional numerical analysis of geocell reinforced soft clay beds by considering the actual geometry of geocell pockets", *Can. Geotech. J.*, **52**(9), 1396-1407.

Hegde, A. and Sitharam, T.G. (2015f), "Use of Bamboo in Soft Ground Engineering and Its Performance Comparison with Geosynthetics: Experimental Studies", *J. Mater. Civil Eng.*, *ASCE*, **27**(9), 1-9.

Hegde, A. and Sitharam, T.G. (2015g), "Experimental and analytical studies on soft clay beds reinforced with bamboo cells and geocells", *Int. J. Geosynth. Ground Eng.*, **1**(2), 1-13.

Hegde, A., Kadabinakatti, S. and Sitharam, T.G. (2014), "Protection of buried pipelines using a combination of geocell and geogrid reinforcement: Experimental studies", *Ground Improv. Geosynth.*, *Geotech. Special Publication-238*, *ASCE*, 289-298.

IS 5249 (1992), Determination of Dynamic Properties of Soil-method of Test; Indian standard, New Delhi, India, 110002.

IS 13301 (1992), Vibration Isolation for Machine Foundations-Guidelines; Indian standard, New Delhi, India, 110002.

Leshchinsky, B. and Ling, H. (2013), "Effects of geocell confinement on strength and deformation behavior of gravel", *J. Geotech. Geoenviron. Eng.*, **139**(2), 340-352.

Madhavi Latha, G. and Somwanshi, A. (2009), "Effect of reinforcement form on the bearing capacity of square plate on sand", *Geotext. Geomembr*, **27**(6), 409-422.

Moghaddas Tafreshi, S.N., Zarei, S.E. and Soltanpour, Y. (2008), "Cyclic loading on foundation to evaluate the coefficient elastic uniform compression in sand", *Proceedings of 14th World Conference on Earthquake Engineering*, Beijing, China, October.

Murthy, V.N.S. (2007), *Advanced Foundation Engineering*, CBS Publishers and Distributors, Bangalore, India.

Pokharel, S.K., Han, J., Leshchinsky, D., Parsons, R.L. and Halahmi, I. (2010), "Investigation of factors influencing behavior of single geocell reinforced bases under static loading", *Geotext. Geomembr*, **28**(6), 570-578.

Rajagopal, K., Krishnaswamy, N.R. and Madhavi Latha, G. (1999), "Behaviour of sand confined with single and multiple geocells", *Geotext. Geomembr*, **17**(3), 171-181.

Sireesh, S., Sitharam, T.G. and Dash, S.K. (2009), "Bearing capacity of circular plate on geocell sand mattress overlying clay bed with void", *Geotext. Geomembr.*, **27**(2), 89-98.

Sireesh, S., Sailesh, P., Sitharam, T.G. and Puppala, A.J (2013), "Numerical analysis of geocell reinforced ballast overlying soft clay subgrades", *Geomech. Eng., Int. J.*, **5**(3), 263-281.

Sitharam, T.G. and Sireesh, S. (2004), "Model studies of embedded circular footing on geogrid reinforced sand beds", *Ground Improv.*, **8**(2), 69-75.

Sitharam, T.G. and Hegde, A. (2013), "Design and construction of geocell foundation to support embankment on soft settled red mud", *Geotext. Geomembr.*, **41**, 55-63.

Sreedhar, M.V. and Goud, P.K. (2011), "Behavior of geosynthetic reinforced sand bed under cyclic loading", *Proceedings of Indian Geotechnical Conference*, Kochi, India, December, pp. 519-522.

Srinivasalu, P. and Vaidyanathan, C.V. (1976), *Handbook of Machine Foundations*, Tata Mcgraw Hill Publishing Company Limited. New Delhi, India.

Srinivasa Murthy, B.R., Sridharan, A. and Bindumadhava (1993), "Evaluation of interface frictional resistance", *Geotext. Geomembr.*, **12**, 235-253.

Tanyu, B.F., Aydilek, A.H., Lau, A.W., Edil, T.B. and Benson, CH (2013), "Laboratory evaluation of geocell-reinforced gravel sub base over poor subgrades", *Geosynth. Int.*, **20**(2), 46-71.

Verma, A.K. and Bhatt, D.R. (2008), "Design of machine foundations on reinforced sand", *Proceedings of 12th International Conference of IACMAG*, Goa, India, October, pp. 3583-3589.

Vesic, A.S. (1973), "Analysis of ultimate loads of shallow foundations", *J. Soil Mech. Found. Div.*, **99**, 45-69.

Viswanadham, B.V.S. and König, D. (2004), "Studies on scaling and instrumentation of geogrid", *Geotext. Geomembr.*, **22**(5), 307-328.

Zreik, D.A., Ladd, C.C. and Germaine, J.T. (1995), "A new fall cone device for measuring the undrained strength of very weak cohesive soils", *Geotech. Test. J.*, **18**(4), 472-482.

CC

List of notations

A	cross sectional area of the plate (m^2)
C_c	coefficient of curvature (dimensionless)
C_u	coefficient of elastic uniform compression (kN/m^3)
C_τ	coefficient of elastic uniform shear (kN/m^3)
C_φ	coefficient of elastic non-uniform compression (kN/m^3)
C_Ψ	coefficient of elastic non-uniform shear (kN/m^3)
D_{10}	effective particle size (mm)
e_{max}	maximum void ratio (dimensionless)
e_{min}	minimum void ratio (dimensionless)
E_v	strain modulus (kPa)
I_f	bearing capacity improvement factor (dimensionless)
K_s	modulus of subgrade reaction (kN/m^3)
m	mass of the foundation system cum the machine assembly (kg)
P	compressive stress (kPa)
q_0	ultimate bearing capacity of the unreinforced soil (kPa)
q_{ult}	ultimate bearing capacity of the reinforced soil (kPa)
Q_0	magnitude of the unbalanced force (kN)
r	radius of the loading plate (m)
S_e	elastic part of the settlement (m)
S_o	settlement of the unreinforced foundation bed (m)
S_r	settlement of reinforced foundation bed (m)
φ	angle of internal friction (degrees)
σ_o	average normal stress below the plate (kPa)
σ_{omax}	maximum average normal stress (kPa)
ω_n	natural frequency of the foundation-soil (rad/s)
ω	operating frequency of the machines (rad/s)